Phase retrieval from speckle patterns of ordering systems

David Montiel, Mark Sutton, and Martin Grant
Physics Department and Centre for the Physics of Materials, McGill University, Rutherford Building, 3600 Rue University, Montréal, Québec, Canada H3A 2T8

(Received 18 June 2009; published 7 October 2009)

The time dependence of the Fourier transform phase of coherently scattered radiation from a system undergoing ordering is studied. Specifically, we derive a simple model that takes into account the known scaling laws for ordering dynamics to predict the statistical behavior of the Fourier transform phase. We consider a two-dimensional system of domains undergoing ordering for both the nonconserved and conserved order-parameter cases (models A and B, respectively). Predictions from our model are compared with numerical experiments, where a time-dependant Ginzburg-Landau equation is integrated to compute the dynamics of the real-space system; then a simple numerical (discrete) Fourier transform is applied to compute the Fourier phase as well as the amplitude (directly related to scattering intensity). An average phase-decorrelation time (the average time it takes for the phase to change by a specific amount) is obtained using both our theoretical model and the numerical results. This quantity is then used to implement a phase-retrieval strategy that consists of measuring scattering intensities of the same nonequilibrium system at different times and then applying an iterative phase-retrieval algorithm (like Fienup's hybrid input-output) recursively with improved initial estimates for faster convergence and higher convergence rates.

DOI: 10.1103/PhysRevE.80.041112 PACS number(s): 64.60.De, 42.30.Rx, 61.05.cc

I. INTRODUCTION

A. Coherent scattering from ordering systems

Scattering of radiation, for example, x-rays, neutrons, or electrons, is a common technique for measuring the microscopic structure of materials. The spatial inhomogeneity of some property in the scattering probe is what makes the incident-beam scatter. The intensity of the resulting scattered beam can then measured in a detector. When the incident radiation is coherent, the measured intensity (in the Born approximation) is related to the magnitude of the Fourier transform of the structure of the sample. If we represent the property that causes the scattering as the field $\psi(\mathbf{r})$, then

$$I(\mathbf{k}) \propto |\hat{\psi}(\mathbf{k})|^2, \tag{1}$$

where $I(\mathbf{k})$ is the measured intensity, $\mathbf{k}$ is the scattering wave vector, and $\hat{\psi}(\mathbf{k})$ is the Fourier transform of $\psi(\mathbf{r})$. In this work, we consider coherent scattering from systems undergoing ordering (kinetics of a first-order phase transition) after a temperature quench. We represent the order parameter as a continuous field $\psi(\mathbf{r})$. The characteristic scattering intensity pattern for these systems features rapidly fluctuating pieces also known as speckle. Typical configuration of domains undergoing ordering and their corresponding speckle patterns at a fixed time τ is shown in Fig. 1.

Ordering is characterized by a well-known dynamic scaling behavior, i.e., patterns at two different times are statistically similar and their properties differ only by a time-dependent factor. This behavior known as the scaling regime usually holds for late times, where domains are well defined and interfaces are relatively sharp. The time dependence of the characteristic length R, which is the only time-dependent quantity, is known to obey a power law of the form $R(\tau)=[B\tau]^n$, where B is a constant and n depends on the conservation laws (or absence thereof) that govern the ordering dynamics. A large number of ordering phenomena fall into two categories (called universality classes): (1) those for which the order parameter is not conserved, called model A, and (2) those for which the order parameter is conserved, called model B. All of the results presented here are obtained for both of these models. The exponent n is known to have a different value for each of these classes. Namely, 1/2 for model A and 1/3 for model B [1–3]. Examples of systems described by model A are the Ising model with flip-spin dynamics and binary alloys undergoing an order-disorder transition. Systems described by model B include the conserved Ising model and binary alloys undergoing spinodal decomposition.

Important properties of a system can be obtained from scattering measurements. In incoherent scattering, for instance, the Fourier transform of the density (or order parameter) correlation function is proportional to the structure factor

$$S(\mathbf{k},\tau) = \langle I(\mathbf{k},\tau)\rangle \propto \hat{C}(\mathbf{k},\tau), \tag{2}$$

where

$$C(\mathbf{r},\tau) = \langle \psi(\mathbf{0},\tau)\psi(\mathbf{r},\tau)\rangle. \tag{3}$$

The brackets in Eqs. (2) and (3) denote ensemble average over initial conditions, which is a way of simulating incoherent scattering. If a system is isotropic then all average properties depend only on the magnitude of the wave vector $k=|\mathbf{k}|$. When the scaling relation holds, one can express $S(\mathbf{k},\tau)$ in terms of a scaling function that depends only on scaled time $t \propto \tau k^{1/n}$,

$$S(k,\tau) = k^{-d}F_1(t). \tag{4}$$

Alternatively, $S(k,\tau)$ can also be expressed in terms of a function of only the scaled wave number k' defined as $k'=kR(\tau)\propto k\tau^n$,

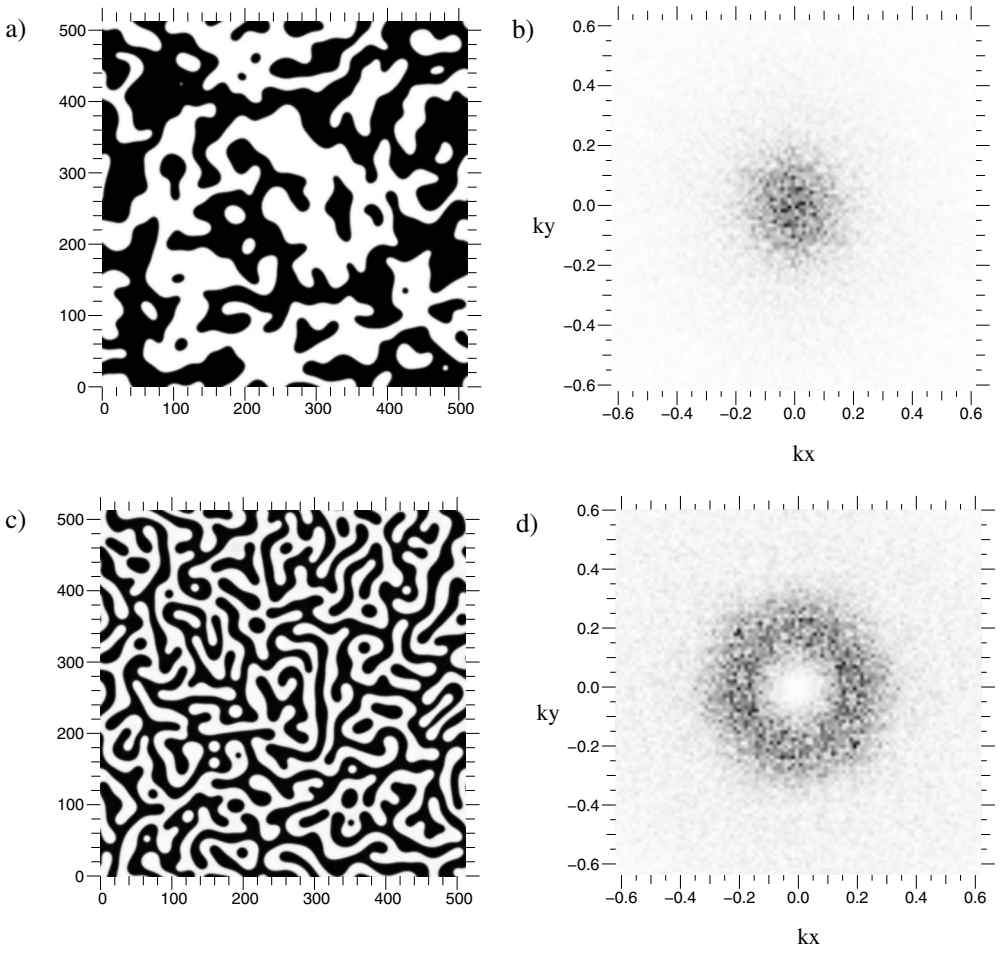

FIG. 1. Examples of 2D phase ordering (numerical simulations with a grid of size 512×512) following a temperature quench. (a) Domain growth (model A) at time $\tau=75$ (in rescaled units). (b) Speckle pattern ($\sqrt{I}$) of system (a) calculated as the modulus of its Fourier transform. (c) Spinodal decomposition (model B) at $\tau=2000$ and (d) speckle pattern ($\sqrt{I}$) of (c).

$$S(k,\tau) = R(\tau)^d F_1'(k'). \tag{5}$$

Equations (2)–(5) are valid for incoherent scattering, where self-averaging takes place and one cannot obtain information about the specific structure (the domains' configuration at a given time) of the system, as opposed to coherent scattering. In the latter case, it can be readily shown that the Fourier transform of the intensity corresponds to the Fourier transform of the autocorrelation function of the order parameter [4], and if, in addition to the intensity, the phase is known (recall that the Fourier transform is in general a complex quantity), then the order-parameter field, or a quantity proportional to it, can also be known via a simple inverse Fourier transform.

B. Phase retrieval

Phase retrieval can be described as the task of obtaining the phase of a function when only the magnitude (modulus) of this function is known. The solution is known to be essentially unique only when the dimensionality of the problem (d) is greater than 1 [5,6]. In order to obtain a unique solution (aside from certain trivial characteristics [7]) for $d \geq 2$, some additional information about the image is needed. This matter, also known as the phase problem, is raised in many fields of interest, such as x-ray crystallography, x-ray, neutron or electron diffraction, and astronomy, when it is often the case that one is only able to measure a quantity related to the magnitude of the Fourier transform of a quantity of interest [8–11].

In the previous section, we described how scattering intensity obtained from experiments relates to spatial properties of the order parameter in the probed system. Namely, Eqs. (1) and (2) relate the intensity to the modulus of the Fourier transform of the order parameter (coherent scattering) and to the structure factor (incoherent scattering), respectively. In this work, we are interested in obtaining the real-space order parameter from the intensity in coherent scattering measurements and the Fourier phase obtained via phase retrieval, i.e., solving the phase problem.

It was also mentioned in the previous section that the coherent scattering intensity provides some information about the structure. However, the intensity alone is insufficient to recover the precise real-space configuration of a system because the phase of the Fourier transform $\hat{\psi}(\mathbf{k})$ is lost, as it cannot be measured in the detector.

In order to obtain the real-space function $\psi(\mathbf{r})$, one needs additional *a priori* information that hopefully can be incor-

porated into a phase-retrieval method. In most cases, some information is available in the form of constraints that are characteristic of the image of study (e.g., positivity, compactness, support, image intensity, or a a combination of these).

Unfortunately, even when enough is known to retrieve the phase in principle, no procedure has been developed that systematically guarantees the solution of the phase problem for all cases. However, several methods have been developed and applied with varying degrees of success. The first important contribution was made by Gerchberg and Saxton [12] in 1972. They developed an algorithm for phase retrieval for cases where both the Fourier and image-space amplitudes are known. Fienup [13] modified the Gerchberg-Saxton algorithm for objects applying support and non-negativity constraints. In 1982, Bates *et al.* developed a method based on the outward recursive propagation of the phase using oversampled measurements of the Fourier transform modulus for compact images [7,14,15]. Again, Fienup [16] in 1982, introduced a set of algorithms, among which the "hybrid input-output" (HIO) is the most widely used in imaging applications. Elser [17] introduced the "difference map" and identified the Fienup algorithms as special cases of the iterated projections method. In general, for all of the algorithms mentioned above, the performance depends on the set of *a priori* constraints available for the particular type of images for which the algorithm is applied.

Most of these methods are iterative, usually use involving an initial guess or estimate of the solution, which is improved recursively until a fixed point is reached. Generally, it has been found, especially in Fienup's methods, that the effectiveness and rate of convergence depend significantly on the initial estimate.

In this work, we propose a phase-retrieval strategy in which an algorithm (we use HIO, but this is not essential) is applied consecutively using simulated intensity data taken at different times of a single instance of ordering dynamics. As we will describe in the following sections, by choosing appropriate time intervals in which to measure we can improve phase retrieval by making better initial guesses taken from previously obtained solutions at "nearby" states. In other words, for a system undergoing spinodal decomposition or domain growth, we propose the use of intensity "snapshots" taken at sufficiently short-time intervals to facilitate phase retrieval when the solution at one or more of these times is known.

In Sec. II we derive a simple theoretical model for phase decorrelation as a function of time during ordering dynamics. In Sec. III we obtain a kind of two-time phase covariance (phase-decorrelation function) from which we calculate a phase-decorrelation time. We compare our numerical and theoretical results. In Sec. IV we apply these results to our phase-retrieval strategy and present an example in which it is applied. Finally, we present our conclusions in Sec. V.

II. MODEL

In this section, we present a simple model to obtain the standard deviation of the phase change between two times of the domains evolution for ordering dynamics. Let there be a system described by order parameter $\psi(\mathbf{r},\tau)$. We consider ordering after a symmetric quench into the coexistence region. In the late time regime, where domains are well defined and of size considerably larger compared to the thickness of interfaces, the value of ψ at a point within one of the domains can be approximated by the equilibrium value of that order parameter under the present set of conditions. For instance, let $\pm\psi_{eq}$, with $\psi_{eq}>0$, be the equilibrium value of the order parameter, then we consider $\psi(\mathbf{r},\tau)\simeq\pm\psi_{eq}$ everywhere except at the interfaces. Furthermore, we neglect the interface thickness.

Within these approximations, we take our system to be described by the field $\psi(\mathbf{r},\tau)$, which can take only the values $\pm\psi_{eq}$. Let $\hat{\psi}(\mathbf{k},\tau)$ be the spatial two-dimensional (2D) Fourier transform of $\psi(\mathbf{r},\tau)$. We can write $\hat{\psi}$ in terms of its modulus A and phase ϕ,

$$\hat{\psi}(\mathbf{k},\tau)=A(\mathbf{k},\tau)e^{\phi(\mathbf{k},\tau)}. \tag{6}$$

As we mentioned in the previous section, at late times of the evolution of domains, the statistical properties of the system depend on time only through a characteristic length $R(t)$. This quantity corresponds to the average domain size.

Because within our approximations, both the magnitude and argument of the Fourier transform are fully determined by the position of the interfaces, then the motion of the interfaces completely determines the time evolution of both modulus and phase. With this in mind, we constructed the simplest possible model that both allows for some analysis and roughly preserves the same features of the real domains in terms of interface motion. We describe this model below, mentioning a few important approximations along the way.

We define our model system $\psi_0(\mathbf{r},\tau)$ to be a set of nonintersecting 2D circles with their centers randomly distributed and with sizes obeying the following time-dependent distribution:

$$n(\kappa)=\alpha\kappa\rho(\kappa), \tag{7}$$

where α is a proportionality constant, $n(\kappa)$ is the proportion of circles of curvature κ (radius $r=1/\kappa$), and $\rho(\kappa)$ is the curvature distribution of the true system, defined in such way that $\rho(\kappa)d\kappa$ is proportional to the total interface length of curvature κ and $\kappa+d\kappa$. The proportionality constant in Eq. (7) can be obtained via the normalization of $n(\kappa)$, which gives $\alpha=1/\langle\kappa\rangle=R$.

We now take the Fourier transform of $\psi_0(\mathbf{r})$. Since this is a linear operator, we can define the quantity $\delta\hat{\psi}_0(\mathbf{k},\kappa)$ as the partial Fourier transform of all circles of curvature between κ and $\kappa+d\kappa$. The value of $\psi_0(\mathbf{k})$ is then

$$\hat{\psi}_0(\mathbf{k})=\int_0^\infty n(\kappa)\delta\hat{\psi}_0(\mathbf{k},\kappa)d\kappa. \tag{8}$$

In a finite system (because the number of circles is a discrete quantity), the integral in Eq. (8) must become a sum.

Our next approximation is that the distribution $n(\kappa)$ is sufficiently sharp and dominated by the mean. In this case, $n(\kappa)=\delta(\kappa-\langle\kappa\rangle)$ and $\hat{\psi}_0(\mathbf{k})=\hat{\psi}_0(\mathbf{k},\kappa)$. Given now that all circles are assumed to be of radius $R=1/\langle\kappa\rangle$, our model sys-

tem $\psi_0(\mathbf{r},\tau)$ is described only by R and the set $\{\mathbf{r}_j\}$ representing the positions of the centers of the circles. Ignoring the constant background term, whose Fourier transform gives a term proportional to $\delta(\mathbf{k})$, we have, for $k \neq 0$,

$$\hat{\psi}_0(\mathbf{k};R,\{\mathbf{r}_j\}) = 2\psi_0 \sum_j \hat{\Pi}(\mathbf{k};R,\mathbf{r}_j), \tag{9}$$

where,

$$\Pi(\mathbf{r};R,\mathbf{r}_j) = \begin{cases} 1 & \text{if } |\mathbf{r}-\mathbf{r}_j| \leq R \\ 0 & \text{otherwise,} \end{cases} \tag{10}$$

corresponds to a circular step function of radius R, centered on $\mathbf{r}_j$. Its Fourier transform is proportional to the Bessel function of the first kind and order one, J_1 with a phase factor determined by the value of $\mathbf{r}_j$,

$$\hat{\Pi}(\mathbf{k};R,\mathbf{r}_j) = \frac{2\pi R}{k} J_1(kR) e^{i\mathbf{k}\cdot\mathbf{r}_j}. \tag{11}$$

Substituting Eq. (11) into Eq. (9), we get

$$\hat{\psi}_0(\mathbf{k};R,\{\mathbf{r}_j\}) = \frac{4\pi\psi_0 R}{k} J_1(kR) \sum_j e^{i\mathbf{k}\cdot\mathbf{r}_j}. \tag{12}$$

The phasor sum on Eq. (12) becomes a random walk in 2D if the positions $\{\mathbf{r}_j\}$ are randomly distributed. Next, we consider a small displacement of the interface, which in our model system corresponds to an expansion or contraction of the circles that constitute it. It is important to stress at this point that we are not modeling our real systems domains to be ψ_0. Rather, we are modeling the displacement of the domains interfaces within a short period of time (for the purpose of phase change) as if it were approximately given by the displacement of the interfaces in our model system. We consider the simplest case of interface displacement that produces an argument change in our model system, which is the uniform expansion or contraction of circles. To the first order, we consider that displacement to be given, in average, by the change in characteristic domain size δR within a short time $\delta\tau$. Thus, each circle is allowed to either randomly contract or expand (but not displace) by $\delta R_j = \pm|\delta R|$. The resulting change in ψ_0 is given by

$$\begin{aligned} \delta\hat{\psi}_0(\mathbf{k};R,\{\mathbf{r}_j\}) &= \hat{\psi}_0(\mathbf{k};\{R+\delta R_j\},\{\mathbf{r}_j\}) - \hat{\psi}_0(\mathbf{k};R,\{\mathbf{r}_j\}) \\ &= 4\pi\psi_0 R J_0(kR) \sum_j e^{i\mathbf{k}\cdot\mathbf{r}_j}\delta R_j \end{aligned} \tag{13}$$

for small values of $|\delta R_j|$. Since the signs of δR_j are random, the sum in Eq. (13) is also a random walk but independent to that of Eq. (12). Seeing both $\hat{\psi}_0$ and $\delta\hat{\psi}_0$ as statistically independent phasors and knowing the variance of the magnitude of each, we can estimate the variance of the phase difference $\delta\phi$

$$\langle\delta\phi^2\rangle \approx 2\left(\frac{\langle|\delta R|\rangle}{R}\right)^2. \tag{14}$$

To obtain Eq. (14), we have, in addition, taken only the lowest-order terms in the expansion of both J_0 and J_1, thus, making it only valid for $kR \ll 1$ (small wave numbers). Note that, for that limit, the above expression is no longer dependent on k. Now we substitute the time dependence into R and δR, given by $R=[B\tau]^n$ and $\delta R \simeq (dR/d\tau)\delta\tau = nB^n\tau^{n-1}\delta\tau$. Substituting in Eq. (13), we get

$$D(\tau,\delta\tau) \equiv \langle\delta\phi^2\rangle^{1/2} = \beta n \bar{\tau}^{-1}\delta\tau, \tag{15}$$

where $\bar{\tau}$ is the average time within the interval $\delta\tau$ and β is a proportionality constant. Equation (15) gives us the rms value of the change in phase as a function of time. It should be valid for small time intervals and small values of kR. Even though many approximations were made in its derivation, Eq. (15) is in fairly good agreement with our numerical results as will be seen in the following sections.

III. NUMERICAL WORK

In this section, we obtain, via numerical simulations, a few important properties to describe the time evolution of the Fourier transform phase during ordering. To obtain ensemble averages of quantities, we perform a set of simulations for systems undergoing ordering after a temperature quench into a coexistence region, varying only initial conditions determined by the thermal noise. We consider the dynamics described by both a nonconserved (model A) and a conserved (model B) order parameter. For each case, we use a deterministic equation that can easily be integrated in time using Euler's method. The derivation of this equation as well as the details of the integration procedures are identical those presented in Ref. [18] for model A and Ref. [19] for model B. As is done in both of these references, thermal noise is neglected throughout the domains' evolution and the source of randomness is the initial state.

In Refs. [18,19], intensity is calculated from the Fourier transform modulus in simulations of ordering dynamics. These results are used to compute the two-time covariance correlation functions to characterize intensity (speckle) fluctuations from the average (whose behavior is well known). In the case of the phase, which is not measurable, its average value (at any time) has no physical meaning; it is only useful when it is known at a particular instance. However, the average rate of change in the phase in time is a useful quantity since it is related to the real-space evolution of the domains. In this work, we compute what we define as the phase-decorrelation function

$$C_{\mathbf{k}}(\mathbf{k},\tau_1,\tau_2) = \langle[\phi(\mathbf{k},\tau_1) - \phi(\mathbf{k},\tau_2)]\rangle^{1/2}. \tag{16}$$

As expected, this quantity can also be collapsed into a scaling function dependent only on scaled times $t_i = Bk^{1/n}\tau_i$ at the late stages of ordering $C_{\mathbf{k}}(\mathbf{k},\tau_1,\tau_2) = C(t_1,t_2)$. By construction $C(t,t)=0$ and increases as Δt increases.

To compute $C(t_1,t_2)$, all simulation parameters (except system size; we took 512) were kept identical to those used in Refs. [18,19] to facilitate comparison of results. The contour plot of the square root of $C(t_1,t_2)$ for models A and B is presented in Fig. 2. These plots are similar to those of two-time intensity covariance presented in Refs. [18,19]. Following their approach, we also substitute t_1 and t_2 by the more natural variables: time average $\bar{t} = (t_1+t_2)/2$ and time differ-

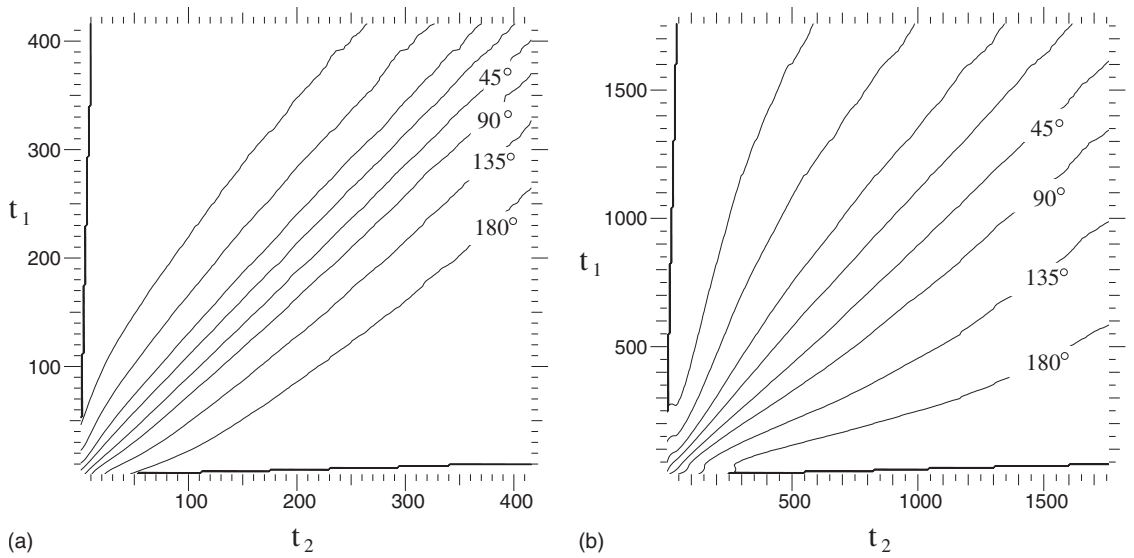

FIG. 2. Contour plots of scaled phase-decorrelation function $C(t_1,t_2)$. (a) Model A (nonconserved) dynamics. (b) Model B (conserved) dynamics. Note that plots are symmetric about the $t_1=t_2$ line since $C(t_2,t_1)=C(t_1,t_2)$.

ence $\delta t=|t_2-t_1|$. We also define a *characteristic* value δt_c that corresponds to the time difference at which $\langle \delta\phi^2\rangle^{1/2}$ has a definite value. In Fig. 3, we plot (again for model A and model B) the characteristic time difference vs average time for $\langle \delta\phi^2\rangle^{1/2}=45°$. We can see that for both cases, at small average times δt_c increases linearly with time. This result agrees with the one obtained with our model on the previous section [note that Eq. (15) remains unchanged if we use rescaled time t instead of τ]. Below, this result is used to obtain time intervals for which the angle decorrelation is constant, as this helps us choose optimal snapshots of the system for phase retrieval.

IV. RESULTS

We now present an example where we incorporate the results obtained in the previous section into our phase-retrieval strategy. The way we proceed is essentially by generating a series of simulated intensity snapshots at time intervals determined with the use of Eq. (15). These snapshots represent measurements at different times of a single undergoing domain growth. We let $\{\tau_j\}$; $j=1,2,\ldots,N_s$ be the set of (rescaled) times at which these snapshots are taken. They are chosen by the following way: the first time τ_1 of the series is chosen to be any time within the late-stage growth regime (where scaling applies and domains are well defined). The next step is to apply Eq. (15) recursively (having chosen a value for the constant β and for D) to obtain the rest of the time series. The last time of the series should be one for which the system possesses a well-defined and relatively simple structure; simple enough to be easily reconstructed (without stagnation) by a standard phase-retrieval method, such as HIO, regardless of the initial guess employed. In the following sample run, where we consider the domain growth (model A) in a 2D system of size 256×256. We let D

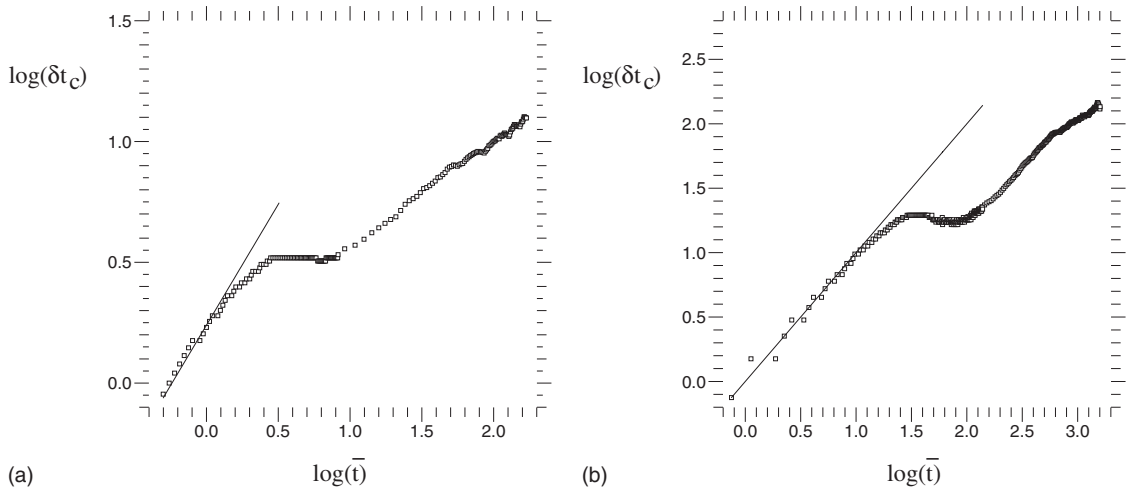

FIG. 3. Characteristic time difference $\log(\delta t_c)$ for $D=\langle \delta\phi^2\rangle^{1/2}=45°$ as a function of average time $\log(\bar{t})$. For both plots, model A (a) and model B (b), the fit for early times (left solid line) has a slope of ≈1, which gives $\delta t_c \propto \bar{t}$.

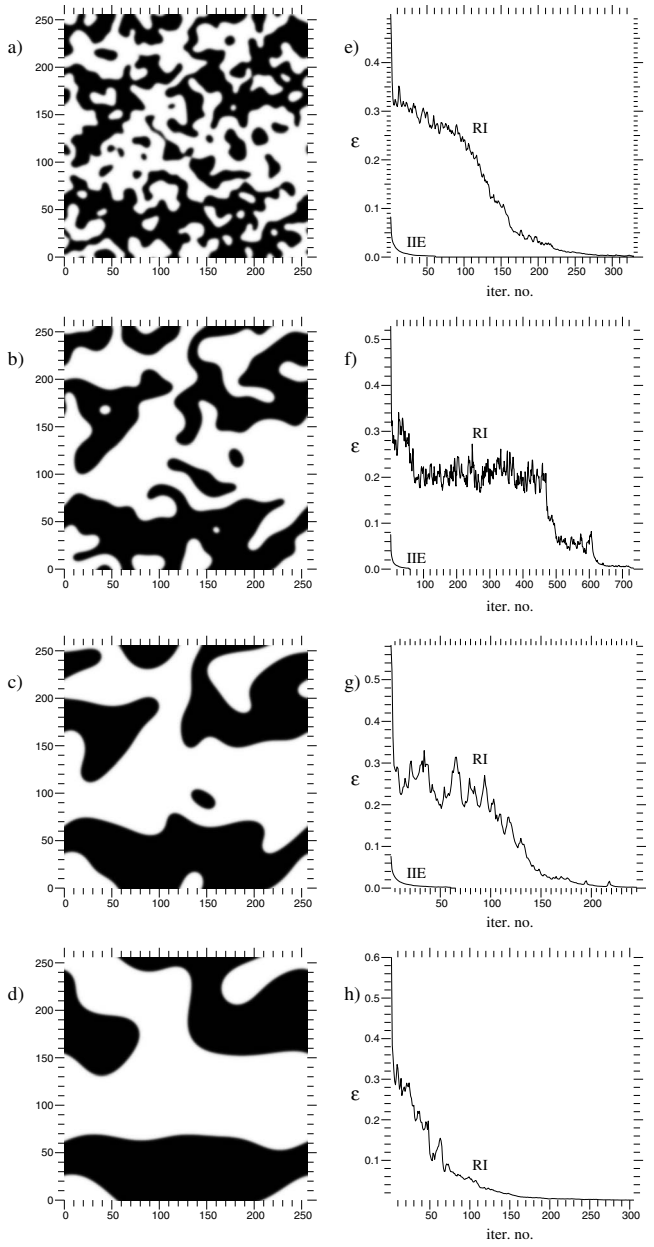

FIG. 4. Patterns of domain growth (model A) after temperature quench, at four different times (a) $\tau=12.5$, (b) $\tau=35.8$, (c) $\tau=122.8$, and (d) $\tau=500$. (e)–(h) Error metric ε vs number of iterations for phase retrieval of the corresponding patterns on the left. Convergence curves for random inputs (RIs) are compared with those using IIEs.

$=45°$ and we obtain the value of β from the plot of Fig. 3(b). In the form of a recursive relation, Eq. (15) [recall that under the approximations of our model, Eq. (15) holds for both τ and t] reads as

$$\tau_{n+1} = \gamma\tau_n, \tag{17}$$

where $\gamma=(2+\epsilon)/(2-\epsilon)$ and $\epsilon=D\beta/n$. Equation (17) shows the times $\{\tau_j\}$ constitute a geometric series. Empirically, we found $\tau_1=12.5$ and $\tau_N=500$ to be appropriate initial and final times. For the value of $\gamma\simeq 1.2$ obtained from the graph, we found that approximately 22 time frames cover the entire

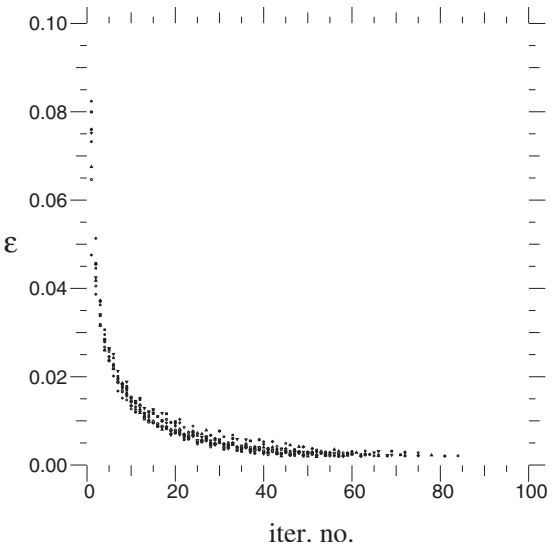

FIG. 5. Overlap of convergence curves, from improved initial estimates, corresponding to different times. Error metric ε vs number of iterations.

time interval. The value of γ was slightly adjusted to $\simeq 1.193$ so that the final frame corresponds to $\tau=500$.

For the final intensity frame, we applied Fienup's HIO algorithm (details of its implementation are given in Ref. [16]) with finite tight support constraints to retrieve the image $\psi(\mathbf{r})$. As initial input image, we used a set of random numbers uniformly distributed between $-\psi_{eq}$ and ψ_{eq}. In what follows, we refer to this initial random guess as random input. Once the phase (and therefore) the image at τ_N was found. We used this image as input (initial estimate) for the HIO algorithm at τ_{N-1}. Because we expect some degree of correlation between the phase at these two times, the input ψ_N must be a better estimate than a random one. Indeed, as we show below, the convergence of the algorithm is much faster in the former case. We repeat this procedure recursively for all time frames until we get to τ_1. In Fig. 4, we compare the error metric (ε) convergence curves obtained with this strategy to the same curves obtained from random inputs. We pick sample intensity snapshots (we show the corresponding order-parameter images instead) at four different times between (and including) τ_1 and τ_N. We found, as Fig. 4 shows, that using the strategy we propose above drastically reduces convergence time for each sample. An interesting finding is that the improved initial estimate (IIE) convergence curves are all approximately the same (they overlap) for different times. Figure 5 shows ensemble averages of IIE curves for the same set of times shown in Fig. 4. Collapse of the data to a single curve is apparent. Empirically, we found the best fit to this curve to be a stretched exponential.

V. CONCLUSIONS

We have, both by a simple model and through numerical simulations, obtained an expression for the average rate of change in the phase of the Fourier transform of the order

parameter in a system undergoing ordering. We have found an expression to estimate the time interval for which the angle statistically decorrelates. This time interval depends on the average time, i.e., the of the domains' evolution. We have devised and applied an effective strategy for phase retrieval that greatly reduces the convergence time of a typical algorithm like Fienup's HIO. We pick intensity snapshots at optimally chosen time intervals that are less than the corresponding decorrelation time. Initially, we solve the phase problem for a late time frame, where the domains have coarsened. Then we use the solution as an initial guess for an earlier more complex frame. This is repeated recursively backward in time. Our method features only one adjustable parameter, which determines an average angular distance between frames. In a real experiment, this strategy's applicability is limited by the rate at which intensity measurements are available. However, the use of experimental data should otherwise be relatively straightforward and it would constitute a good test for the practical application of this technique.

ACKNOWLEDGMENTS

This work was supported by the Natural Sciences and Engineering Research Council of Canada and Le Fonds Québécois de la Recherche sur la Nature et les Technologies.

[1] J. D. Gunton, M. S. Miguel, and P. S. Sahni, in *Phase Transitions and Critical Phenomena*, edited by C. Domb and J. L. Lebowitz (Academic, London, 1983), Vol. 8.
[2] P. C. Hohenberg and B. I. Halperin, Rev. Mod. Phys. **49**, 435 (1977).
[3] A. J. Bray, Adv. Phys. **43**, 357 (1994).
[4] D. W. Ricker, *Echo Signal Processing* (Springer, New York, 1983).
[5] Y. M. Bruck and L. G. Sodin, Opt. Commun. **30**, 304 (1979).
[6] M. H. Hayes, IEEE Trans. Acoust., Speech, Signal Process. **30**, 140 (1982).
[7] R. H. T. Bates, Optik (Stuttgart) **61**, 247 (1982).
[8] J. C. Dainty and J. R. Fienup, in *Image Recovery: Theory and Application*, edited by H. Stark (Academic Press, New York, 1987), pp. 231–275.
[9] W. Kim and M. H. Hayes, Proceedings of the Acoustics, Speech, and Signal Processing (ICASSP-91) (IEEE Computer Society, Washington, D.C., 1991), p. 1765.
[10] D. Sayre and H. N. Chapman, Acta Crystallogr., Sect. A: Found. Crystallogr. **51**, 237 (1995).
[11] V. Elser, Acta Crystallogr., Sect. A: Found. Crystallogr. **55**, 489 (1999).
[12] R. W. Gerchberg and W. O. Saxton, Optik (Stuttgart) **35**, 237 (1972).
[13] J. R. Fienup, Opt. Lett. **3**, 27 (1978).
[14] K. L. Garden and R. H. T. Bates, Optik (Stuttgart) **62**, 131 (1982).
[15] W. R. Fright and R. H. T. Bates, Optik (Stuttgart) **62**, 219 (1982).
[16] J. R. Fienup, Appl. Opt. **21**, 2758 (1982).
[17] V. Elser, J. Opt. Soc. Am. A Opt. Image Sci. Vis **20**, 40 (2003).
[18] G. Brown, P. A. Rikvold, M. Sutton, and M. Grant, Phys. Rev. E **56**, 6601 (1997).
[19] G. Brown, P. A. Rikvold, M. Sutton, and M. Grant, Phys. Rev. E **60**, 5151 (1999).